DOI: 10.1002/ejic.200600859

The Complexes $[OsCl_2(azole)_2(dmso)_2]$ and $[OsCl_2(azole)(dmso)_3]$: Synthesis, Structure, Spectroscopic Properties and Catalytic Hydration of Chloronitriles

Iryna N. Stepanenko,[a] Berta Cebrián-Losantos,[a] Vladimir B. Arion,*[a] Artem A. Krokhin,[a] Alexey A. Nazarov,[a] and Bernhard K. Keppler*[a]

Keywords: Osmium / N ligands / Homogeneous catalysis / Hydration

Two families of mixed-ligand osmium(II) complexes, namely *trans*,*cis*,*cis*-$[Os^{II}Cl_2(azole)_2(dmso)_2]$ [azole = indazole (**1**), pyrazole (**2**), benzimidazole (**3**) and imidazole (**4**)] and *cis*,*fac*-$[Os^{II}Cl_2(azole)(dmso)_3]$ [azole = indazole (**5**), pyrazole (**6**), benzimidazole (**7**) and imidazole (**8**)] have been prepared by taking advantage of the destabilising *trans* effect of the *S*-bonded dmso ligands. These complexes have been characterised by microanalysis, IR, UV/Vis, ^1H and ^{13}C NMR spectroscopy, electrospray mass spectrometry, cyclic voltammetry and X-ray crystallography. They have been found to catalyse the hydration of trichloroacetonitrile to trichloroacetamide and dichloroacetonitrile to dichloroacetamide with high selectivity. The catalyst efficiency depends strongly on the nature of the complex and the azole ligand present. The highest turnover (TON of 412 for trichloroacetamide and 578 for dichloroacetamide) and product yield (82.7 % for trichloroacetamide and 75.3 % for dichloroacetamide) have been achieved with complex **7**.

Introduction

The coordination chemistry of dimethyl sulfoxide has been the subject of intensive studies in the past[1–3] and continues to attract the attention of researchers today.[4,5] Of the platinum group metals, the most extensively studied appear to be ruthenium-dmso complexes, some of which are endowed with potent antitumour properties[6,7] or have found application in catalytic processes.[8–10] In addition, Ru^{II}-dmso complexes have been successfully employed as precursors for the synthesis of a large variety of compounds, and, in particular, of $[Ru^{II}Cl_2(azole)_2(dmso)_2]$ geometric isomers,[11–16] with $[Ru^{II}Cl_2(4\text{-}NO_2Him)_2(dmso)_2]$ possessing radiosensitising properties. Quite recently, we discovered that *trans*,*trans*,*trans*-$[RuCl_2(Hind)_2(dmso)_2]$ (s in italics means coordination via sulfur) and *trans*,*cis*,*cis*-$[RuCl_2(Hind)_2(dmso)_2]$ species are able to mediate the insertion of the C≡N group of acetonitrile in the N1–H bond of the N2-coordinated indazole, these being the first examples of the metal-assisted iminoacylation of indazole.[17]

Comparison of the chemistry of ruthenium(II) dmso complexes with that of osmium(II) dmso species has permitted us to unravel expected similarities between these two types of complexes, but also remarkable, although less pronounced, differences. In particular, both ruthenium(II) and osmium(II) have been shown to form *cis*,*fac*-$[MCl_2(dmso)(dmso)_3]$ and *trans*-$[MCl_2(dmso)_4]$ isomers, the first of which contains three facially S-coordinated dmso ligands and one dmso molecule O-ligated to the metal ion, with the second containing four S-coordinated dmso ligands. However, the third (linkage) isomer *cis*-$[MCl_2(dmso)_4]$, with all dmso ligands coordinated via sulfur, has been isolated only for osmium(II).[18] In addition, it should be noted that despite the similarity between ruthenium(II) dmso and osmium(II) dmso complexes, the latter have, in general, rarely been used as precursors in inorganic synthesis. Examples reported in the literature have been confined to reactions of *trans*-$[OsCl_2(dmso)_4]$, *trans*-$[OsBr_2(dmso)_4]$ or *cis*,*fac*-$[OsCl_2(dmso)(dmso)_3]$ with chelating ligands containing Te, Sb or P as donor atoms.[19–21] This observed difference in the number of documented reactions can probably, in part, be explained by stronger Os–L bonds and higher ligand substitution activation energies in comparison with the case of ruthenium analogues.[22] In addition, it must be stressed that the position of the two metals in the periodic table is important, but not sufficient for the successful synthesis of the desired osmium complexes. This cannot be performed in a routine way simply by following the protocols for ruthenium species, and very often particular skills and experience are required. With this in mind, we set out to use the Os^{II} dmso isomers available as starting compounds and to study their reactivity toward azole heterocycles, especially indazole (Hind), pyrazole (Hpz), benzimidazole (Hbzim) and imidazole (Him; see Scheme 1).

[a] Institute of Inorganic Chemistry, Faculty of Chemistry, University of Vienna,
Währingerstr. 42, 1090 Vienna, Austria
Fax: +43-1-4277-52680
E-mail: vladimir.arion@univie.ac.at
bernhard.keppler@univie.ac.at

Supporting information for this article is available on the WWW under http://www.eurjic.org or from the author.

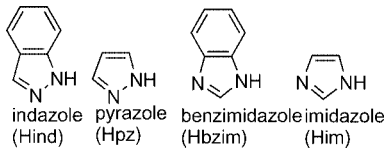

Scheme 1.

We anticipated (i) the isolation of "pure" isomers of composition [$OsCl_2$(azole)$_2$(dm*so*)$_2$], due to the distinct kinetic inertness of Os^{II} complexes over Ru^{II} species, without any competing isomerisation reactions interfering, (ii) the isolation of other species, the formation of which under similar reaction conditions does not occur in the case of ruthenium analogues, and (iii) the elucidation of previously unknown facets of the reactivity profile of the compounds prepared. In particular, in order to establish the scope of the recently discovered metal-assisted iminoacylation of indazole,[17] we checked the reactivity of the isolated *trans*,*cis*,*cis*-[$Os^{II}Cl_2$(Hind)$_2$(dm*so*)$_2$] isomer towards CH_3CN and CCl_3CN. We show that no insertion of the C≡N group into the N1–H bond of the N2-coordinated indazole takes place. Instead, with trichloroacetonitrile we observed hydration of this solvent and set out to examine this reaction in more detail.

Herein we report the synthesis of two different families of compounds, namely *trans*,*cis*,*cis*-[$Os^{II}Cl_2$(azole)$_2$(dm*so*)$_2$] [azole = Hind (**1**), Hpz (**2**), Hbzim (**3**), Him (**4**)] and *cis*,*fac*-[$OsCl_2$(azole)(dm*so*)$_3$] [azole = Hind (**5**), Hpz (**6**), Hbzim (**7**) and Him (**8**)] and their structural and spectroscopic characterisation both in the solid state and in solution. In addition, the results of the study of the hydration reaction of chloronitriles catalysed by the prepared complexes are reported.

Results and Discussion

Synthesis

While treatment of *trans*-[$OsCl_2$(dm*so*)$_4$] with two equivalents of azole ligand in boiling absolute ethanol afforded the isomers *trans*,*cis*,*cis*-[$OsCl_2$(azole)$_2$(dm*so*)$_2$] (**1**–**4**) in 80–88% yield (Scheme 2), the reaction under similar conditions starting from *cis*-[$OsCl_2$(dmso)$_4$] resulted in the formation of complexes *cis*,*fac*-[$OsCl_2$(azole)(dm*so*)$_3$] (**5**–**8**) in 46–85% yield. We also discovered that heating complexes **1**–**4** in dimethyl sulfoxide at 125 °C led to their conversion into **5**–**8**, respectively, in 70–75% yield. It should be noted that the synthesis of ruthenium analogues of **5**–**8** is possible under mild conditions by selective replacement of the *O*-bonded dmso in *cis*,*fac*-[$RuCl_2$(dm*so*)(dm*so*)$_3$] by treatment with a stoichiometric amount of the corresponding azole ligand.[12,15a,16b] If, however, the azole ligand is added in excess and the reaction is carried out at elevated temperatures, isomers of the composition [$RuCl_2$(azole)$_2$(dm*so*)$_2$] are produced.[13,14,15a]

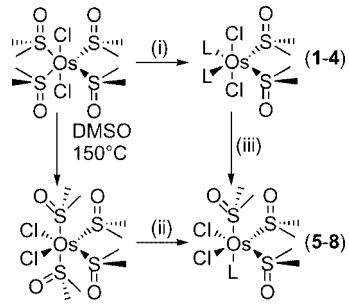

Scheme 2. Synthesis of complexes *trans*,*cis*,*cis*-[$OsCl_2L_2$(dm*so*)$_2$] [L = Hind (**1**), Hpz (**2**), Hbzim (**3**), Him (**4**)] and *cis*,*fac*-[$OsCl_2L$(dm*so*)$_3$] [L = Hind (**5**), Hpz (**6**), Hbzim (**7**) and Him (**8**)]. Reaction conditions: (i) 2 equiv. L, EtOH, 80–87 °C, 1–3 h; (ii) 2 equiv. L, EtOH, 80–87 °C, 40 min–2 h; (iii) dmso, 125 °C, 45 min–2 h. The complex *trans*-[$OsCl_2$(dm*so*)$_4$] at 150 °C undergoes isomerisation into *cis*-[$OsCl_2$(dmso)$_4$] in dmso.[21]

The formation of **1**–**4** from *trans*-[$OsCl_2$(dm*so*)$_4$] and **5**–**8** from *cis*-[$OsCl_2$(dmso)$_4$] can be explained by a remarkable destabilising *trans* effect of the *S*-bonded dmso molecules. The *trans* and *cis* isomers have two and one of these destabilising vectors, respectively, therefore substitution at these sites predetermined by structural differences between the isomers is favoured. Two pathways for the conversion of **1**–**4** into **5**–**8** can be proposed (Scheme 3): (a) the azole ligand is substituted by a molecule of dmso to give *trans*,*mer*-[$OsCl_2$(azole)(dm*so*)$_3$], which then isomerises to *cis*,*fac*-[$OsCl_2$(azole)(dm*so*)$_3$]; (b) another four isomers can theoretically exist along with *trans*,*cis*,*cis*-[$OsCl_2$(azole)$_2$(dm*so*)$_2$]. Taking into account that the *cis*,*cis*,*trans* and *cis*,*trans*,*cis* isomers have not been reported for ruthenium,[17] we postulate that the formation or emergence of the other two isomers (*trans*,*trans*,*trans* and *cis*,*cis*,*cis*) is more likely. Substitution of one of the two azole ligands by dmso, followed by isomerisation, results in *cis*,*fac*-[$OsCl_2$(azole)(dm*so*)$_3$]. The intermediate species could not be identified by the analyti-

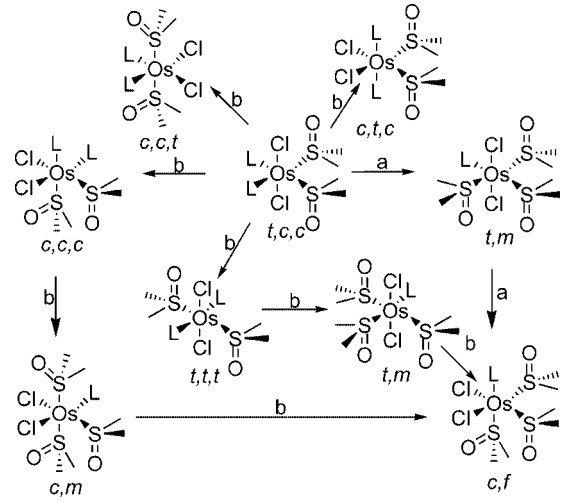

Scheme 3. Proposed transformation pathways (a and b) of **1**–**4** into **5**–**8**. Abbreviations used: *c* – *cis*, *t* – *trans*, *m* – *mer*, *f* – *fac*.

cal techniques available and the mechanism of this transformation remains uncertain. Nevertheless, the first pathway is shorter and simpler, which makes it more plausible.

^{1}H and ^{13}C NMR Spectra

In the ^{1}H NMR spectra of **1/5** and **3/7** one set of signals of equal intensity for the Hind and Hbzim ligands [at δ = 12.74, 8.68, 7.65, 7.47, 7.40 and 7.16 ppm (**1**); δ = 14.43, 9.20, 7.73, 7.51, 7.43 and 7.19 ppm (**5**); δ = 12.87, 8.41, 7.87, 7.47, 7.13 and 6.91 ppm (**3**); δ = 13.18, 8.78, 8.21, 7.59, 7.29 and 7.24 ppm (**7**)] is observed. Likewise, one set of ^{13}C resonances is seen for Hind in **1** and **5** and Hbzim in **3** and **7**. In addition, the singlet at δ = 3.37 (**1**) and 3.27 ppm (**3**), of sixfold intensity in comparison to the indazole or benzimidazole proton resonances present in the spectra, was assigned to the dmso methyl protons coordinated to osmium(II) via sulfur. Note that the downfield shift of dmso protons when coordinated through oxygen is much less with respect to the metal-free dmso.[18] In *cis*-[OsCl$_2$(dms*o*)(dm*s*o)$_3$], for example, this signal is observed at δ = 2.76 ppm. In the ^{13}C NMR spectrum the dmso resonance is present at δ = 45.4 (**1**) and 45.6 ppm (**3**). Two resonances in the ^{1}H NMR spectrum at δ = 3.64 and 3.35 ppm, with a 2:1 relative intensity in **5**, and three signals of equal intensity at δ = 3.59, 3.45 and 3.28 ppm in **7**, are indicative of the presence of three dmso ligands coordinated through sulfur. Three resonances for *S*-bonded dmso ligands at δ = 48.8, 48.1 and 45.8 (**5**) and 48.9, 47.1 and 45.7 ppm (**7**) are seen in the ^{13}C NMR spectra of **5** and **7**. This is in agreement with the C_2 symmetry of **1** and **3** and the C_1 symmetry of **5** and **7** in solution. Significant downfield shifts of the resonances of the protons nearest to the Os^{II} centre (NH and C3-H) in **1** and **5** with respect to the position of the same signals for the metal-free indazole (δ = 10.01 and 8.09 ppm) and in **3** and **7** with respect to the position of the NH, C2-H and C4-H/C7-H signals for the metal-free benzimidazole (δ = 12.44, 8.21 and 7.61 ppm) are also worthy of note.

The presence of singlet resonances at δ = 3.34 (**2**), 3.13 (**4**), 3.60, 3.59 and 3.29 (**6**), and 3.51, 3.45 and 3.25 ppm (**8**) in the ^{1}H NMR spectra of **2**, **4**, **6** and **8** indicates coordination of the dmso ligands to osmium(II) through sulfur. In the ^{13}C NMR spectra the resonances of the dmso carbon atoms are found at δ = 45.6 (**2**), 45.5 (**4**), 48.7, 47.9 and 45.8 (**6**) and 48.5, 47.2 and 46.0 ppm (**8**). Four signals for the pyrazole and imidazole protons and three carbon resonances in **2**, **4**, **6** and **8** (see Experimental Section) are indicative of the C_2 symmetry of molecules of **2** and **4** and the C_1 symmetry of **6** and **8** in solution. As for **1**, **3**, **5** and **7**, significant downfield shifts of the resonances of the protons nearest to the Os^{II} centre (NH and C3-H in **2** and **6** and NH, C2-H and C4-H in **4** and **8**) with respect to the position of the same signals for the metal-free pyrazole [δ = 10.26 (NH) and 7.63 ppm (C3-H and C5-H)] and imidazole [δ = 12.03 (NH), 7.64 (C2-H) and 7.01 ppm (C4-H and C5-H)] are observed.

Crystal Structures of 1–8

The asymmetric unit of **1** contains two crystallographically distinct [Os^{II}Cl$_2$(Hind)$_2$(dm*s*o)$_2$] molecules **1A** (Figure 1) and **1B** (Figure S1). Selected bond lengths and angles are listed in Table 1. Essentially octahedral coordination around the osmium atom is found in both molecules. The two chlorido ligands are mutually *trans*, while the two dmso and the two indazole ligands are correspondingly *cis* coordinated to each other. Thus, the configuration of the two independent complexes can be described as *trans*,*cis*,*cis*-[Os^{II}Cl$_2$(Hind)$_2$(dm*s*o)$_2$]. The Os–Cl bond lengths [2.4138(12) and 2.3984(11) Å in **1A** and 2.3989(12) and 2.4127(12) Å in **1B**] are similar to the Ru–Cl bond lengths in two independent molecules of *trans*,*cis*,*cis*-[Ru^{II}Cl$_2$(Hind)$_2$-(dm*s*o)$_2$] [2.4105(7), 2.4137(7), 2.4069(7) and 2.4147(7) Å], whereas the Os–S bond lengths [2.2250(11) and 2.2453(11) in **1A** and 2.2460(11) and 2.2245(11) Å in **1B**] are somewhat shorter than the Ru–S bond lengths [2.2439(13), 2.2588(8), 2.2477(7) and 2.2578(14) Å] and the Os–N interatomic distances [2.130(4), 2.137(4) (**1A**) and 2.122(4), 2.139(3) Å (**1B**)] are slightly longer than the Ru–N distances [2.1177(18), 2.1255(14), 2.1159(14) and 2.1244(19) Å]. The orientation of the *cis*-arranged indazole ligands in **1A** can be described by the torsion angles $\Theta_{Cl2–Os1–N1–N2}$ [17.5(3) °] and $\Theta_{Cl2–Os1–N3–N4}$ [–0.1(3)°] and is stabilised by the intramolecular hydrogen bonds N2–H2···Cl2 (N2–H2 0.880, H2···Cl2 2.572, N2···Cl2 3.115 Å; N2–H2–Cl2 120.69°) and

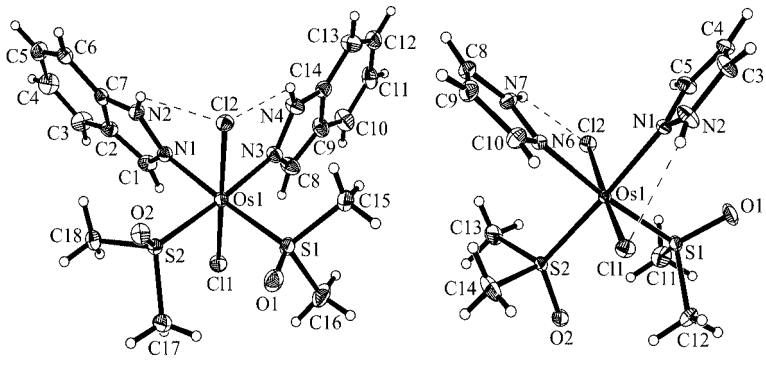

Figure 1. Molecular structures of the first independent molecule *trans*,*cis*,*cis*-[Os^{II}Cl$_2$(Hind)$_2$(dm*s*o)$_2$] (**1A**; left) and *trans*,*cis*,*cis*-[Os^{II}Cl$_2$(Hpz)$_2$(dm*s*o)$_2$] (**2**; right), showing the atom-numbering schemes. Thermal ellipsoids are drawn at the 50% probability level.

Table 1. Selected bond lengths [Å] and angles [°] in **1** and **2**.

	1A	**1B**	**2**
Os1–N1/Os2–N5	2.130(4)	2.122(4)	2.1202(17)
Os1–N3/Os2–N7	2.137(4)	2.139(3)	
Os1–N6			2.1365(17)
Os1–S1/Os2–S3	2.2250(11)	2.2460(11)	2.2498(6)
Os1–S2/Os2–S4	2.2453(11)	2.2245(11)	2.2386(6)
Os1–Cl1/Os2–Cl3	2.4138(12)	2.4127(12)	2.4293(8)
Os1–Cl2/Os2–Cl4	2.3984(11)	2.3989(12)	2.4053(8)
S1–O1/S3–O3	1.490(4)	1.489(3)	1.4819(17)
S2–O2/S4–O4	1.492(3)	1.495(3)	1.4855(16)
N1–Os1–N3/N5–Os2–N7	84.79(15)	86.42(14)	
N1–Os1–N6			86.03(6)
S1–Os1–S2/S3–Os2–S4	91.47(4)	91.01(4)	94.51(2)
Cl1–Os1–Cl2/Cl3–Os2–Cl4	176.23(4)	174.94(4)	174.556(17)

N4–H4A···Cl2 (N4–H4A 0.880, H4A···Cl2 2.530, N4···Cl2 3.086 Å; N4–H4A–Cl2 121.78°). The water molecules are involved in a number of hydrogen-bonding interactions with coordinated dmso and indazole molecules that stabilise the crystal lattice.

The X-ray diffraction study of **2** showed that the complex has a distorted octahedral geometry around the central metal ion (Figure 1). As in **1**, the two chlorido ligands are *trans* to each other, with Os1–Cl1 and Os1–Cl2 bond lengths of 2.4293(8) and 2.4053(8) Å, respectively. Two pyrazole ligands bind in a monodentate fashion with a *cis* arrangement [Os1–N1 2.1202(17) and Os1–N6 2.1365(17) Å] and the remaining positions of the coordination polyhedron are occupied by dmso ligands through the Os–S bond [Os1–S1 2.2498(6) and Os1–S2 2.2386(6) Å]. Intramolecular hydrogen bonding is evident between N2 and Cl1 [N2–H2 0.880, H2···Cl1 2.531, N2···Cl1 3.098 Å; N2–H2–Cl1 122.87°] and between N7 and Cl2 [N7–H7 0.880, H7···Cl2 2.518, N7···Cl2 3.086 Å; N7–H7–Cl2 123.00°]. These determine the orientation of the pyrazole rings, which can be described by the torsion angles $\Theta_{Cl1–Os1–N1–N2}$ [–12.59(15) °] and $\Theta_{Cl2–Os1–N6–N7}$ [3.67(14)°].

The results of X-ray diffraction studies of **3** and **4** are shown in Figure 2. Selected bond lengths and angles are listed in Table 2.

Table 2. Selected bond lengths [Å] and angles [°] in **3** and **4**.

	3	**4**
Os1–N1	2.146(2)	2.138(4)
Os1–N3	2.138(3)	2.120(5)
Os1–S1	2.2273(7)	2.2166(12)
Os1–S2	2.2282(8)	2.2254(11)
Os1–Cl1	2.4170(8)	2.402(2)
Os1–Cl2	2.4142(8)	2.428(3)
S1–O1	1.480(2)	1.495(4)
S2–O2	1.481(2)	1.482(5)
N1–Os1–N3	83.44(9)	84.25(17)
S1–Os1–S2	90.22(3)	91.42(4)
Cl1–Os1–Cl2	175.69(3)	175.24(10)

The X-ray diffraction study of **5**–**8** revealed that the the Os^{II} ion in all these complexes has a distorted octahedral geometry (see Figures 3 and 4). The coordination sites of osmium(II) are occupied by three sulfur atoms of three dmso molecules, one N atom of the corresponding azole heterocycle and two Cl^- ligands, which are arranged *cis* to each other. Selected bond lengths and angles are given in Table 3. For the axial dmso and azole molecules the Cl2–Os1–S1 and Cl2–Os1–N1 bond angles are 89.53(4)° and 84.83(9)° (**5**), 89.52(3)° and 84.02(9)° (**6**), 91.55(3)° and 85.00(7)° (**7**) and 92.40(3)° and 85.68(6)° (**8**), respectively,

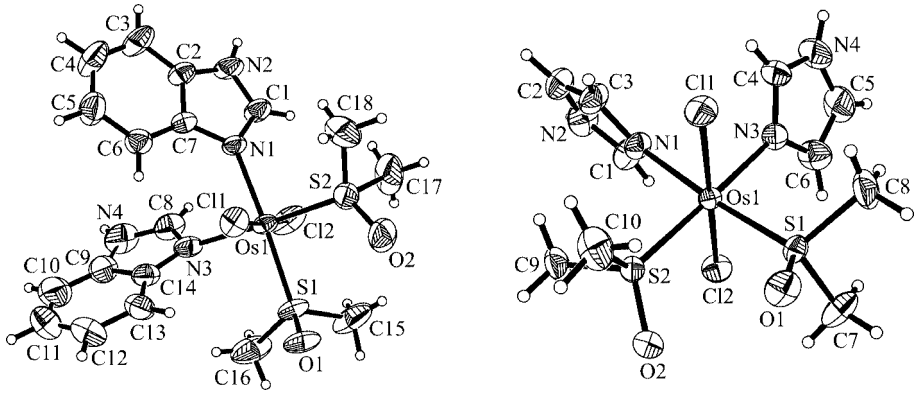

Figure 2. Molecular structures of *trans*,*cis*,*cis*-[$Os^{II}Cl_2$(Hbzim)$_2$(dmso)$_2$] (**3**; left) and *trans*,*cis*,*cis*-[$Os^{II}Cl_2$(Him)$_2$(dmso)$_2$] (**4**; right), showing the atom-numbering schemes. Thermal ellipsoids are drawn at the 50% probability level.

thus indicating notable steric constraints of the axial dmso group, which is pushed towards the chlorido ligands. The S2–Os1–S3 bond angle is 90.95(4)°, 91.40(4)°, 97.16(3)° and 93.55(3)° in **5**–**8**, respectively, while the Cl1–Os1–Cl2 angle of 86.41(3)°, 86.78(4)°, 86.92(3)° and 85.98(3)°, respectively, deviates more significantly from the ideal value of 90°. The $\Theta_{Cl2–Os1–N1–N2}$ torsion angle of –33.9°, which describes the orientation of the indazole ring in **5**, is probably determined by the bifurcated hydrogen bond between N2 and Cl2 [N2–H2 0.880, H2···Cl2 2.596, N2···Cl2 3.056 Å; N2–H2–Cl2 113.53°] and O2(x + 1/2, –y + 2, z) [N2–H2 0.880, H2···O2 2.247, N2···Cl2 2.999 Å; N2–H2–O2 143.27°]. The significant difference (ca. 35 σ) in the bond lengths between Os1 and the two equatorial dmso ligands in **5** can probably be explained, in part, by the involvement of these dmso ligands in two different strong hydrogen-bonding interactions, the former with a lattice ethanol molecule [O4–H4 0.840, H4···O3(x + 1/2, –y + 1, z) 1.921, O4···O3 2.753 Å; O4–H4–O3 170.49°] and the latter with N2 of the neighbouring indazole ligand (vide supra). The orientation of the pyrazole ring in **6** is determined by the intramolecular hydrogen bonding between N2 of the pyrazole and O3 of the

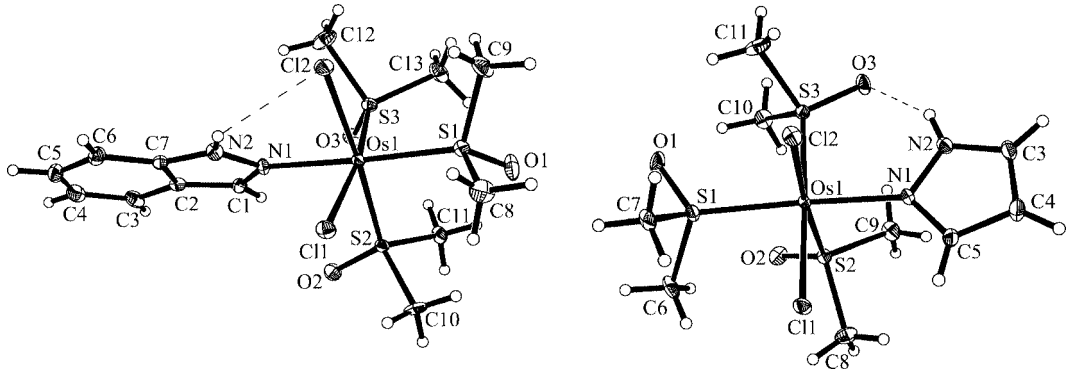

Figure 3. Molecular structures of *cis*,*fac*-[$Os^{II}Cl_2$(Hind)(dm*so*)$_3$] (**5**; left) and *cis*,*fac*-[$Os^{II}Cl_2$(Hpz)(dm*so*)$_3$] (**6**; right), showing the atom-numbering scheme. Thermal ellipsoids are drawn at the 50% probability level.

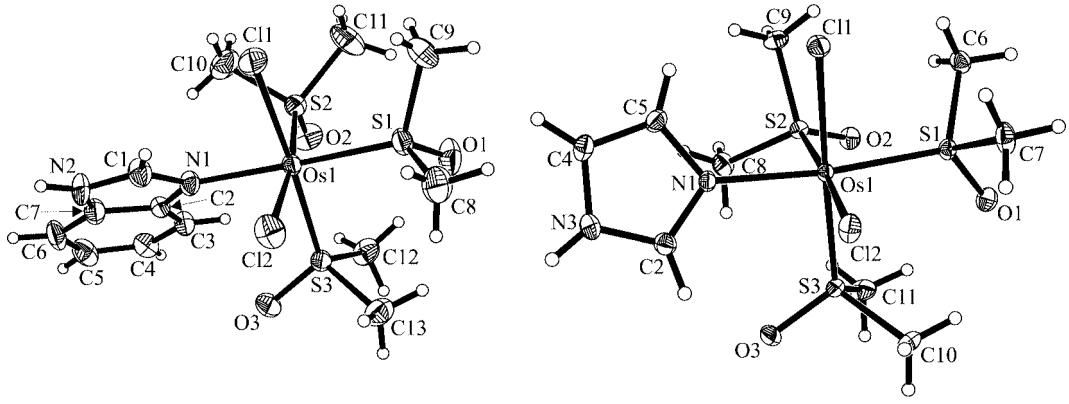

Figure 4. Molecular structures of *cis*,*fac*-[$Os^{II}Cl_2$(Hbzim)(dm*so*)$_3$] (**7**; left) and *cis*,*fac*-[$Os^{II}Cl_2$(Him)(dm*so*)$_3$] (**8**; right), showing the atom-numbering schemes. Thermal ellipsoids are drawn at the 50% probability level.

Table 3. Selected bond lengths [Å] and angles [°] in **5**–**8**.

	5	**6**	**7**	**8**
Os1–N1	2.136(3)	2.131(3)	2.150(2)	2.148(2)
Os1–S1	2.2821(10)	2.2982(9)	2.2878(8)	2.2901(7)
Os1–S2	2.2899(8)	2.2638(9)	2.2746(7)	2.2276(7)
Os1–S3	2.2480(9)	2.2570(12)	2.2804(7)	2.2807(7)
Os1–Cl1	2.4302(10)	2.4326(12)	2.4202(7)	2.4245(7)
Os1–Cl2	2.4232(8)	2.4229(9)	2.4364(8)	2.4335(7)
S1–O1	1.475(4)	1.486(3)	1.477(2)	1.4850(19)
S2–O2	1.481(3)	1.485(3)	1.472(2)	1.4926(18)
S3–O3	1.492(3)	1.501(2)	1.482(2)	1.4861(18)
S1–Os1–Cl1	92.07(4)	85.97(3)	89.86(3)	87.22(2)
N1–Os1–Cl1	84.24(8)	86.88(7)	86.47(7)	85.06(6)
S2–Os1–S3	90.95(4)	91.40(4)	97.16(3)	93.55(3)
Cl1–Os1–Cl2	86.41(3)	86.78(4)	86.92(3)	85.98(3)

dmso ligand [N2–H2 0.880, H2···O3 1.850, N2···O3 2.635 Å; N2–H2–O3 147.58°], which results in a small $\Theta_{S3-Os1-N1-N2}$ torsion angle of 4.1(3)°. The imidazole ligand in **8** is hydrogen bonded to lattice ethanol [N3–H3 0.880, H3···O4(–*x* + 1, –*y*, –*z* + 2) 1.917, N3···O4 2.771 Å; N3–H3–O4 163.16°], which, in turn, acts as a hydrogen-bond donor to one of the dmso ligands [O4–H4 0.840, H4···O2 1.897, O4···O2 2.735 Å; O4–H4–O2 175.04°].

Electrochemical Study

The electrochemical properties of osmium(II) complexes **1**, **2**, **5** and **6** and **3**, **4**, **7** and **8** were studied by cyclic voltammetry in acetonitrile (0.15 M [*n*Bu_4N][BF_4]) and dmf (0.15 M [*n*Bu_4N][BF_4]), respectively. Voltammetric data are given in Table 4, and the cyclic voltammogram of **2** is shown in Figure 5. One oxidative response is found for all complexes. Taking into account the similar responses in the analogous ruthenium complexes,[17] these electron-transfer processes are assigned to Os^{II}–Os^{III} oxidation.

Table 4. Cyclic voltammetric data for **1**–**8**[a] and their estimated redox potential values.

	$E_{1/2}^{ox}$ found[b,c] [V vs. NHE]	$E_{1/2}^{red}$ calcd. [V vs. NHE]
1[d]	0.94 (60)	0.79
2[d]	0.89 (60)	0.67
3[e]	0.80 (70)	0.61
4[e]	0.71 (60)	0.51
5[d]	1.66 (65)	1.10
6[d]	1.57 (60)	1.04
7[e]	1.51 (70)	1.01
8[e]	1.40 (60)	0.96

[a] Supporting electrolyte: [*n*Bu_4N][BF_4]; scan rate: 0.2 V s^{-1}. [b] $E_{1/2} = 0.5(E_{pa} + E_{pc})$, where E_{pa} and E_{pc} are the anodic and cathodic peak potential, respectively. [c] $\Delta E_p = E_{pa} - E_{pc}$ [mV]. [d] In acetonitrile. [e] In dmf.

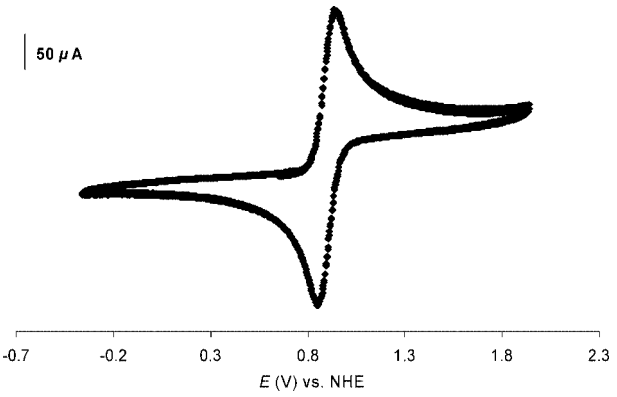

Figure 5. Cyclic voltammogram of *trans*,*cis*,*cis*-[$Os^{II}Cl_2$(Hpz)$_2$(dmso)$_2$] in acetonitrile solution (0.15 M [*n*Bu_4N][BF_4]) at a scan rate of 0.2 V s^{-1}.

The oxidation potentials for **1**–**4** (0.94–0.71 V) are markedly lower than those for **5**–**8** (1.66–1.40 V), which is in agreement with the stronger net electron-acceptor character of the S-coordinated dmso as compared with the azole ligands, which are more effective σ-donors. In addition, the redox potentials of the complexes are in the following order in the two series of compounds: $E_{1/2}^{ox}$(**1**, **5**) > $E_{1/2}^{ox}$(**2**, **6**) > $E_{1/2}^{ox}$(**3**, **7**) > $E_{1/2}^{ox}$(**4**, **8**), which agrees with the relative electron-donor character of the N-ligands [E_L(Hind) > E_L(Hpz) > E_L(Hbzim) > E_L(Him)] and their basicity [pK_a(Hind) < pK_a(Hpz) < pK_a(Hbzim) < pK_a(Him)[23]). The responses are reversible or quasi-reversible and are characterised by a peak-to-peak separation (ΔE_p) of 60–70 mV and an anodic peak current (i_{pa}) that is almost equal to the cathodic peak current (i_{pc}) (or slightly different), as expected for reversible electron-transfer processes. The one-electron nature of the observed oxidation was verified by comparing its current height (i_{pa}) with that of a standard ferrocene/ferrocenium couple under identical experimental conditions.

The $E_{1/2}^{ox}$ values for complexes **1**–**4** and **5**–**8** are larger than those expected on the basis of the general Lever equation, by using the known values of S_m and I_m (1.01 and –0.40, respectively) for the Os^{II}/Os^{III} redox couple and the E_L values for the various ligands [E_L(Cl) = –0.24, E_L(dmso) = 0.57,[24] E_L(Hind) = 0.26, E_L(Hpz) = 0.20, E_L(Hbzim) = 0.17, E_L(Him) = 0.12[25]) due to the influence of the stereochemistry on the electronic distribution in the complexes.

The Reactivity of Complexes 1–8 Towards Nitriles

Recently we have reported the first example of a ruthenium(II)-mediated coupling reaction of acetonitrile with 1*H*-indazole.[17] We found that the reaction of *trans*,*cis*,*cis*-[$Ru^{II}Cl_2$(Hind)$_2$(dmso)$_2$] with acetonitrile at room temperature proceeds with displacement of one indazole ligand from the coordination sphere of ruthenium and formation of an amidine ligand isolated as [$Ru^{II}Cl_2${HN=C(Me)-ind}(dmso)$_2$]·H_2O. As a logical consequence of this finding we studied the behaviour of the osmium analogue *trans*,*cis*,*cis*-[$Os^{II}Cl_2$(Hind)$_2$(dmso)$_2$] (**1**) and complexes **2**, **5** and **6** in acetonitrile. No amidine formation was observed in an acetonitrile solution of **1** at room temperature after five days. Even after heating the solutions of **1**, **2**, **5** and **6** at 80 °C for 1–2 h the complexes remained intact and could be recovered after evaporation of acetonitrile at reduced pressure, as verified by ^{1}H NMR spectroscopy. It should, however, be noted that the solutions become coloured both at room temperature and on heating, although the minor species responsible for this colour change could not be identified. It is known[26] that the direct synthesis of amidines from a nitrile and an amine can be realised when the nitrile is activated by a strong electron-acceptor group such as CCl_3. With this in mind, we studied the reactivity of complexes **1** and **2** towards trichloroacetonitrile. Heating the solutions of **1** and **2** in CCl_3CN/methanol (1:1, v/v) at 65 °C for 1 h, CCl_3CN/hexane (1:6, v/v) at 80 °C for 2 h or prolonged refluxing (up to 16 h) of compounds **1** and **2** in neat CCl_3CN at 85 °C did not result in the desired amidine. Removal of the volatiles after the reaction of **2** with neat CCl_3CN left a solid residue, which was washed with diethyl

ether. This solid was shown by ^{1}H NMR spectroscopy to contain the starting complex **2**. On slow evaporation of the diethyl ether washing solution a few colourless crystals separated, which proved to be suitable for an X-ray diffraction study. The determined cell parameters were in excellent agreement with those documented in the literature for trichloroacetamide.[27] Being intrigued by this disclosure, we decided to find out whether complexes **1**–**8** might play a catalytic role in the hydration of trichloroacetonitrile to give trichloroacetamide.

Catalytic Hydration of Chloronitriles by 1–8

Trichloroacetamide and its derivatives exhibit fungicidal,[28] germicidal,[29] cardiovascular[30] and antitumour[31] activity. In addition, some of them are used as insect chemosterilants[32] or nitrification inhibitors.[33] They are also important agents and building blocks in preparative organic chemistry,[34] and, in particular, in peptide synthesis.[35] Although the synthetic approaches to trichloroacetamide are well-optimised,[36] they usually require the use of ammonia gas, which means that a route based on the catalytic hydration of trichloroacetonitrile would appear to be more appealing and environmentally friendly (Scheme 4).

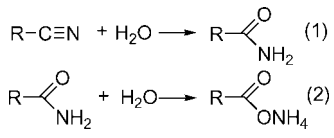

Scheme 4.

The selective hydration of nitriles to carboxamides is currently an important laboratory and industrial reaction.[37,38] The conversion of acrylonitrile into acrylamide, which is an important industrial reagent, for instance, is of considerable practical significance.[38,39] Such reactions are often base or acid catalysed. The main disadvantage of these catalysts is that the undesirable further hydrolysis of carboxamides into carboxylic acids (or their salts) occurs [Equation (2) in Scheme 4]. To avoid such a scenario transition metal complexes should be used in neutral conditions. Complexes **1**–**8** exhibit catalytic activity in the hydration of trichloroacetonitrile in solution. In our model reaction, we converted trichloroacetonitrile into trichloroacetamide and ammonium trichloroacetate. In the control experiments, the hydration of trichloroacetonitrile was carried out in the absence of osmium(II) complexes. A small amount of CCl_3CONH_2 (0.6%) was detected after the reaction of 1 mL of trichloroacetonitrile with 1.3 mL of water at 75 °C for 24 h. These conditions were found to be optimal for catalytic hydration of acetonitrile to acetamide by other osmium(II) compounds.[40] Depending on the azole ligands present in complexes **1**–**8**, the yields of the main product trichloroacetamide varied from 1.05 to 82.72%, with turnover numbers (TON) ranging from 6.22 to 412 (Table 5). The selectivity of formation of this product is remarkable (Table 5). The yields of ammonium trichloroacetate are commonly rather low and do not exceed 0.3%.

Complexes **5**–**8**, which contain three dmso ligands, are more efficient hydration catalysts than **1**–**4**, which contain two coordinated dmso ligands. Complexes **3** and **4** exhibit higher catalytic activity than **1** and **2**. Analogously, compounds **7** and **8** are significantly more efficient catalysts than **5** and **6**. It is worth noting that **7** shows the highest catalytic activity, with a turnover that is an order of magnitude higher than the second best catalyst and with good selectivity. Experiments with the hydrolysis of $CHCl_2CN$ mediated by complex **7** gave the following yields (%) and TON values for $CHCl_2CONH_2$ and $CHCl_2COONH_4$: 75.3, 578 and 1.7, 12.7, while those with CH_2ClCN as substrate in the presence of the same complex afforded $CH_2ClCONH_2$ in a very low yield (2.2%) with low TON value (22) and the ammonium salt of monochloroacetate in 0.48% yield and very low turnover (TON = 5). The catalytic activity of the starting compound *trans*-[$OsCl_2$(dm*s*o)$_4$] has not been studied since its NMR spectrum showed full decomposition after heating the reaction mixture at 75 °C for 1 h.

Compounds **1**–**8** have no free coordination site to allow either water or trichloroacetonitrile binding to Os^{II}. As a possible mechanism for nitrile hydration we propose the substitution of one of the dmso molecules in light of the fact that traces of free dmso are found in the NMR spectra after performing the catalytic reaction. It should also be noted that *cis*,*fac*-[$RuCl_2$(Hind)(dm*s*o)$_3$] has been shown to

Table 5. Comparison of some catalysts for the hydrolysis of trichloroacetonitrile at 75 ± 1 °C.[a]

Complex	Yield of CCl_3CONH_2 [mg (%)]	Turnover number	Yield of CCl_3COONH_4 [mg (%)]	Turnover number	Molar ratio CCl_3CONH_2/ CCl_3COONH_4
1	17 (1.1)	6.2 ± 0.4	2.4 (0.13)	0.8 ± 0.2	7.9
2	18.5 (1.2)	6.4 ± 0.1	3.6 (0.20)	1.1 ± 0.2	5.7
3	28 (1.7)	10.5 ± 0.1	3.2 (0.18)	1.1 ± 0.1	9.7
4	109 (6.7)	36.4 ± 0.4	2.2 (0.12)	0.6 ± 0.1	55.0
5	53 (3.3)	19.4 ± 0.1	0.9 (0.05)	0.3 ± 0.1	65.3
6	103.5 (6.4)	35.0 ± 2.1	2.4 (0.13)	0.7 ± 0.1	47.9
7	1090 (82.7)	412 ± 30	5.4 (0.30)	1.8 ± 0.1	224.2
8	147 (9.1)	49 ± 3	1.2 (0.07)	0.3 ± 0.1	136.0

[a] When the experiment was performed without catalyst under identical conditions (1 mL of CCl_3CN and 1.3 mL of triply distilled water at 75 °C for 24 h), no more than 10 mg (0.6%) of CCl_3CONH_2 was obtained.

undergo replacement of indazole by acetonitrile at room temperature with formation of *cis*,*fac*-[$RuCl_2$(MeCN)-(dm*so*)$_3$].[17] This suggests another possible catalytic pathway for chloronitrile hydration, but does not explain the different efficiency of catalysts **5**–**8**. The catalytic nitrile hydration mechanism proposed by Chottard et al.[41] for cobalt(III) complexes with sulfenato-S ligands under mildly acidic conditions exploits the nucleophilic properties of coordinated sulfenates. This might be another option for osmium(II) sulfoxide-S complexes as well. Density functional calculations on the subject are currently underway in our laboratory.

Conclusions

Two novel families of osmium(II) complexes, namely *trans*,*cis*,*cis*-[$OsCl_2$(azole)$_2$(dm*so*)$_2$] and *cis*,*fac*-[$OsCl_2$-(azole)(dm*so*)$_3$], have been prepared and characterised by exploring the destabilising *trans* effect of *S*-bonded dmso ligands to osmium in *trans*-[$Os^{II}Cl_2$(dm*so*)$_4$] and *cis*-[Os^{II}-Cl_2(dmso)$_4$]. In both series of complexes osmium(II) shows a preference for sulfur binding. In contrast to their ruthenium congeners, the complexes *trans*,*cis*,*cis*-[$OsCl_2$(Hind)$_2$-(dm*so*)$_2$] and *cis*,*fac*-[$OsCl_2$(Hind)(dm*so*)$_3$] do not undergo a coupling reaction with acetonitrile to give amidine chelate formation. Instead, complexes **1**–**8** have been found to catalyse the selective hydration of trichloroacetonitrile to trichloroacetamide, and dichloroacetonitrile to dichloroacetamide. The more acidic complexes of the type *cis*,*fac*-[$OsCl_2$(azole)(dm*so*)$_3$] commonly show higher activity than *trans*,*cis*,*cis*-[$OsCl_2$(azole)$_2$(dm*so*)$_2$]. In addition, the catalyst efficiency is also dependent on the azole ligand bonded to osmium(II). The highest yields (82.7 and 75.3%) and turnovers (TON values 412 and 578), with high selectivity for trichloroacetamide and dichloroacetamide, respectively, have been achieved with *cis*,*fac*-[$OsCl_2$(Hbzim)(dm*so*)$_3$]. These preliminary results are interesting and inspire us to investigate the hydration of acrylonitrile (where the selectivity is often not high), since the vinyl group resembles the $CHCl_2$ group in its electron-withdrawing ability.

Experimental Section

General: The synthesis of all complexes was performed under an atmosphere of dry argon, using standard Schlenk techniques. *trans*-[$OsCl_2$(dm*so*)$_4$] and *cis*-[$OsCl_2$(dmso)$_4$] were prepared according to literature protocols.[18]

***trans*,*cis*,*cis*-[$OsCl_2$(Hind)$_2$(dm*so*)$_2$] (1):** A suspension of indazole (0.10 g, 0.85 mmol) and *trans*-[$OsCl_2$(dm*so*)$_4$] (0.20 g, 0.35 mmol) in dry ethanol (10 mL) was stirred at room temperature for 1 h and then heated at 80 °C for a further hour. The yellow-green solution was concentrated by evaporating part of the solvent off under reduced pressure until a yellow solid separated. The product was filtered off, washed with diethyl ether and dried in vacuo. Yield: 0.18 g (80%). $C_{18}H_{24}Cl_2N_4O_2OsS_2$ (653.64): calcd. C 33.08, H 3.70, N 8.57, S 9.81; found C 33.11, H 3.73, N 8.39, S 9.60. MS (ESI^+): *m*/*z* 677 $[M + Na]^+$; (ESI^-): *m*/*z* 653 $[M - H]^-$. IR (CsI): $\tilde{\nu}$ = 253 and 273 m ν(Os–N) and σ(Os–N–C); 315 m ν(Os–Cl); 382 m σ(C–S–O); 433 and 451 s ν(Os–S); 1018, 1072 s and 1091 vs ν(*S*–O); 1239 m, 1356 s, 1423, 1510 and 1627 m ν(C–C), ν(C–N) and σ(C–H); 3040, 3070 and 3125 w ν(C–H); 3239 and 3303 cm^{-1} s ν(N–H). UV/Vis (MeOH): λ_{max} (ε) = 210 nm (63676 $M^{-1}cm^{-1}$), 240 sh (18469), 277 (32733), 290 sh (29318), 302 sh (22529), 345 (5264). ^1H NMR (400.13 MHz, $CDCl_3$): δ = 12.74 (s, 2 H, NH), 8.68 (s, 2 H, CH=N), 7.65 (d, *J* = 8.0 Hz, 2 H, C4-H), 7.47 (d, *J* = 8.0 Hz, 2 H, C7-H), 7.40 (t, *J* = 7.3 Hz, 2 H, C6-H), 7.16 (t, *J* = 7.3 Hz, 2 H, C5-H), 3.37 (s, 12 H, CH_3) ppm. $^{13}C\{^1H\}$ NMR (100.63 MHz, $CDCl_3$): δ = 139.9 (C8), 135.5 (C3), 128.9 (C6), 122.6 (C9), 122.4 (C5), 121.3 (C4), 110.4 (C7), 45.4 (CH_3) ppm. Single crystals suitable for X-ray structure analysis were crystallised from an ethanol solution saturated with diethyl ether.

***trans*,*cis*,*cis*-[$OsCl_2$(Hpz)$_2$(dm*so*)$_2$] (2):** A suspension of pyrazole (0.05 g, 0.73 mmol) and *trans*-[$OsCl_2$(dm*so*)$_4$] (0.20 g, 0.35 mmol) in dry ethanol (10 mL) was stirred at room temperature for 2 h and then heated at 80 °C for a further 2 h. The yellow-green solution was concentrated under reduced pressure until a yellow solid separated. The product was filtered off, washed with diethyl ether and dried in vacuo. Yield: 0.16 g (85%). $C_{10}H_{20}Cl_2N_4O_2OsS_2$ (553.52): calcd. C 21.70, H 3.64, N 10.12, S 11.58; found C 21.67, H 3.43, N 9.82, S 11.49. MS (ESI^+): *m*/*z* 577 $[M + Na]^+$; (ESI^-): *m*/*z* 553 $[M - H]^-$. IR (CsI): $\tilde{\nu}$ = 217, 232 and 254 m ν(Os–N) and σ(Os–N–C); 319 m ν(Os–Cl); 394 m σ(C–S–O); 432 s and 451 m ν(Os–S); 1009 s, 1048, 1082 vs and 1127 s ν(*S*–O); 1353, 1411, 1471 and 1518 m ν(C–C), ν(C–N) and σ(C–H); 2926, 3018 w and 3126 m ν(C–H); 3286 and 3317 cm^{-1} s ν(N–H). UV/Vis (MeOH): λ_{max} (ε) = 232 nm (37020 $M^{-1}cm^{-1}$), 278 sh (8503), 344 (757). ^1H NMR (400.13 MHz, $CDCl_3$): δ = 13.05 (s, 2 H, NH), 7.83 (t, *J* = 2.0 Hz, 2 H, C3-H), 7.65 (t, *J* = 1.8 Hz, 2 H, C5-H), 6.40 (q, *J* = 2.3 Hz, 2 H, C4-H), 3.34 (s, 12 H, CH_3) ppm. $^{13}C\{^1H\}$ NMR (100.62 MHz, $CDCl_3$): δ = 139.1 (C3), 129.8 (C5), 106.4 (C4), 45.6 (CH_3) ppm. X-ray diffraction quality crystals of **2** were grown from ethanol solution.

***trans*,*cis*,*cis*-[$OsCl_2$(Hbzim)$_2$(dm*so*)$_2$] (3):** A suspension of benzimidazole (0.04 g, 0.35 mmol) and *trans*-[$OsCl_2$(dm*so*)$_4$] (0.10 g, 0.17 mmol) in dry ethanol (5 mL) was heated at 87 °C for 1.5 h. The solution was then cooled to room temperature. The yellow solid was collected by filtration, washed with ethanol (2 × 1 mL) and dried in vacuo. Yield: 0.10 g (88%). $C_{18}H_{24}Cl_2N_4O_2OsS_2$ (653.67): calcd. C 33.07, H 3.70, N 8.57, S 9.81; found C 33.05, H 3.73, N 8.52, S 9.55. MS (ESI^+): *m*/*z* 677 $[M + Na]^+$, 559 $[OsCl_2$-(Hbzim)(dm*so*)$_2$ + $Na]^+$; (ESI^-): *m*/*z* 535 $[OsCl_2$(Hbzim)(dm*so*)$_2$ – $H]^-$, 457 $[OsCl_2$(Hbzim)(dm*so*) – $H]^-$. IR (CsI): $\tilde{\nu}$ = 243 and 280 m ν(Os–N) and σ(Os–N–C); 307 m ν(Os–Cl); 397 m σ(C–S–O); 432 and 461 s ν(Os–S); 970, 1010 and 1063 b vs ν(*S*–O); 1247, 1271, 1306, 1421, 1464, 1505 and 1624 m ν(C–C), ν(C–N) and σ(C–H); 2921 and 3143 m ν(C–H); 3261 and 3410 cm^{-1} s ν(N–H). UV/Vis (MeOH): λ_{max} (ε) = 272 nm (24415 $M^{-1}cm^{-1}$), 278 (22390). ^1H NMR (400.13 MHz, [D_6]dmso): δ = 12.87 (s, 2 H, NH), 8.41 (s, 2 H, CH=N), 7.87 (d, *J* = 8.4 Hz, 2 H, C4-H), 7.47 (d, *J* = 8.00 Hz, 2 H, C7-H), 7.13 (t, *J* = 7.5 Hz, 2 H, C6-H), 6.91 (t, *J* = 7.5 Hz, 2 H, C5-H), 3.27 (s, 12 H, CH_3) ppm. $^{13}C\{^1H\}$ NMR (100.62 MHz, [D_6]dmso): δ = 147.4 (C2), 142.3 (C8 or C9), 133.2 (C8 or C9), 123.7 (C6), 122.2 (C5), 120.9 (C4), 113.1 (C7), 45.6 (CH_3) ppm. X-ray diffraction quality crystals of **3**·CH_3CN were obtained from a solution of **3** in acetonitrile.

***trans*,*cis*,*cis*-[$OsCl_2$(Him)$_2$(dm*so*)$_2$] (4):** Imidazole (0.036 g, 0.53 mmol) was added to a solution of *trans*-[$OsCl_2$(dm*so*)$_4$] (0.15 g, 0.26 mmol) in dry ethanol (10 mL) and the reaction mixture heated at 87 °C for 3 h. After cooling the solution to room temperature, the brown solid was filtered off, washed with ethanol

(3 × 3 mL) and dried in vacuo. Yield: 0.13 g (88%). $C_{10}H_{20}Cl_2N_4O_2OsS_2$ (553.56): calcd. C 21.69, H 3.64, N 10.12, S 11.58; found C 21.90, H 3.55, N 9.82, S 11.39. MS (ESI$^+$): *m/z* 577 [M + Na]$^+$, 509 [$OsCl_2$(Him)(dm*so*)$_2$ + Na]$^+$; (ESI$^-$): *m/z* 553 [M – H]$^-$, 485 [$OsCl_2$(Him)(dm*so*)$_2$ – H]$^-$. IR (CsI): $\tilde{\nu}$ = 219, 258 and 274 m ν(Os–N) and σ(Os–N–C); 315 m ν(Os–Cl); 393 m σ(C–S–O); 433 and 455 s ν(Os–S); 1003, 1056 bs and 1140 s ν(*S*–O); 1292, 1309, 1326, 1432, 1498 and 1541 m ν(C–C), ν(C–N) and σ(C–H); 2924, 2963 and 3060 ν(C–H); 3137 b and 3455 cm^{-1} sh ν(N–H). UV/Vis (MeOH): λ_{max} (ε) = 223 nm (23993 M^{-1} cm^{-1}), 349 (787). ^{1}H NMR (400.13 MHz, [D$_6$]dmso): δ = 12.44 (s, 2 H, NH), 8.14 (s, 2 H, CH=N), 7.38 (s, 2 H, C4-H), 7.10 (s, 2 H, C5-H), 3.13 (s, 12 H, CH_3) ppm. ^{13}C{^{1}H} NMR (100.62 MHz, [D$_6$]dmso): δ = 138.4 (C2), 128.3 (C4), 116.4 (C5), 45.5 (CH_3) ppm. X-ray diffraction quality crystals were obtained from a solution of **4** in ethanol.

***cis*,*fac*-[$OsCl_2$(Hind)(dm*so*)$_3$] (5). Method (a):** A suspension of indazole (0.045 g, 0.38 mmol) and *cis*-[$OsCl_2$(dmso)$_4$] (0.10 g, 0.18 mmol) in dry ethanol (10 mL) was heated at 80 °C for 40 min. The resulting colourless solution was cooled to room temperature and then concentrated by partial evaporation of the solvent under reduced pressure. The white product that separated was filtered off, washed with diethyl ether and dried in vacuo. Yield: 0.09 g (80%).

Method (b): A yellow-green solution of **1** (0.10 g, 0.15 mmol) in dimethyl sulfoxide (5 mL) was heated slowly to 125 °C and maintained at this temperature for 45 min. After evaporation of the solvent under reduced pressure at 100–110 °C, the white or light-grey residue was washed with a small amount of dry ethanol and diethyl ether and dried in vacuo. Yield: 0.07 g (75%). $C_{13}H_{24}Cl_2N_2O_3OsS_3$ (613.63): calcd. C 25.45, H 3.94, N 4.57, S 15.67; found C 25.56, H 3.96, N 4.56, S 15.68. MS (ESI$^+$): *m/z* 637 [M + Na]$^+$; (ESI$^-$): *m/z* 613 [M – H]$^-$. IR (CsI): $\tilde{\nu}$ = 226 and 256 m ν(Os–N) and σ(Os–N–C); 281 and 307 m ν(Os–Cl); 385 m σ (C–S–O); 441 and 471 s ν(Os–S); 953, 1024, 1048 s, 1091 and 1112 vs ν(*S*–O); 1217, 1315, 1365, 1416, 1516 and 1631 m ν(C–C), ν(C–N) and σ(C–H); 2928 and 3023 m ν(C–H); 3069, 3123 and 3144 cm^{-1} w ν(N–H). UV/Vis (MeOH): λ_{max} (ε) = 215 nm (20945 M^{-1} cm^{-1}), 234 sh (6460), 268 sh (7947), 288 (9910), 305 sh (7531), 342 (428). ^{1}H NMR (400.13 MHz, $CDCl_3$): δ = 14.43 (s, 1 H, NH), 9.20 (s, 1 H, CH=N), 7.73 (d, *J* = 8.0 Hz, 1 H, C4-H), 7.51 (d, *J* = 8.0 Hz, 1 H, C7-H), 7.43 (t, *J* = 7.5 Hz, 1 H, C6-H), 7.19 (t, *J* = 7.5 Hz, 1 H, C5-H), 3.64 (s, 12 H, CH_3), 3.35 (s, 6 H, CH_3) ppm. ^{13}C{^{1}H} NMR (100.62 MHz, $CDCl_3$): δ = 140.4 (C8), 137.2 (C3), 129.2 (C6), 122.8 (C9), 122.6 (C5), 121.5 (C4), 110.9 (C7), 48.8 (CH_3), 48.1 (CH_3), 45.8 (CH_3) ppm. Crystals of **5**·C_2H_5OH suitable for X-ray structure analysis were obtained from an ethanol solution of **5**.

***cis*,*fac*-[$OsCl_2$(Hpz)(dm*so*)$_3$] (6). Method (a):** A suspension of pyrazole (0.025 g, 0.37 mmol) and *cis*-[$OsCl_2$(dmso)$_4$] (0.10 g, 0.18 mmol) in dry ethanol (10 mL) was heated at 80 °C for 1 h. The resulting colourless solution was cooled to room temperature and then concentrated by partial evaporation of the solvent under reduced pressure. The white product that separated was filtered off, washed with diethyl ether and dried in vacuo. Yield: 0.08 g (85%).

Method (b): A yellow-green solution of **2** (0.10 g, 0.18 mmol) in dimethyl sulfoxide (5 mL) was heated slowly to 125 °C and maintained at this temperature for 45 min. After evaporation of the solvent under reduced pressure the remaining white solid was washed with a small amount of dry ethanol and diethyl ether and dried in vacuo. Yield: 0.07 g (70%). $C_9H_{22}Cl_2N_2O_3OsS_3$ (563.57): calcd. C 19.18, H 3.93, N 4.97, S 17.07; found C 19.32, H 3.88, N 4.93, S 17.09. MS (ESI$^+$): *m/z* 587 [M + Na]$^+$; (ESI$^-$): *m/z* 563 [M – H]$^-$. IR (CsI): $\tilde{\nu}$ = 234 and 254 m ν(Os–N) and σ(Os–N–C); 277 and 305 s ν(Os–Cl); 384 s σ (C–S–O); 429 and 470 s ν(Os–S); 935 s, 971 m, 1017 vs, 1062 m and 1098 vs ν(*S*–O); 1299 w, 1362 m, 1414 s and 1553 m ν(C–C), ν(C–N) and σ(C–H); 2807, 2922 and 3007 m ν(C–H); 3026, 3108 and 3126 cm^{-1} m ν(N–H). UV/Vis (MeOH): λ_{max} (ε) = 213 nm sh (15689 M^{-1} cm^{-1}), 232 sh (11458), 296 (1165), 341 sh (194). ^{1}H NMR (400.13 MHz, $CDCl_3$): δ = 14.44 (s, 1 H, NH), 8.60 (t, *J* = 1.8 Hz, 1 H, C3-H), 7.66 (t, *J* = 1.8 Hz, 1 H, C5-H), 6.40 (q, *J* = 2.3 Hz, 1 H, C4-H), 3.60 (s, 6 H, CH_3), 3.59 (s, 6 H, CH_3), 3.29 (s, 6 H, CH_3) ppm. ^{13}C{^{1}H} NMR (100.62 MHz, $CDCl_3$): δ = 140.7 (C3), 130.7 (C5), 107.3 (C4), 48.7 (CH_3), 47.9 (CH_3), 45.8 (CH_3) ppm. Crystals of **6** suitable for X-ray structure analysis were grown from ethanol solution.

***cis*,*fac*-[$OsCl_2$(Hbzim)(dm*so*)$_3$] (7). Method (a):** Benzimidazole (0.038 g, 0.32 mmol) was added to a solution of *cis*-[$OsCl_2$-(dmso)$_4$] (0.086 g, 0.17 mmol) in dry ethanol (9 mL) and the reaction mixture heated at 87 °C for 1 h. After the solution had cooled to room temperature, the white solid was filtered off, washed with ethanol (3 × 5 mL) and dried in vacuo. Yield: 0.055 g (60%).

Method (b): A solution of **3** (0.07 g, 0.11 mmol) in dimethyl sulfoxide (2.5 mL) was heated slowly to 125 °C and maintained at this temperature for 1.5 h. The solvent was removed under reduced pressure and the white residue washed with a small amount of absolute ethanol and diethyl ether and dried in vacuo. Yield: 0.05 g (75%). $C_{13}H_{24}Cl_2N_2O_3OsS_3$ (613.67): calcd. C 25.44, H 3.94, N 4.56, S 15.67; found C 25.23, H 3.83, N 4.46, S 15.40. MS (ESI$^+$): *m/z* 637 [M + Na]$^+$; (ESI$^-$): *m/z* 613 [M – H]$^-$, 535 [$OsCl_2$(Hbzim)(dm*so*)$_2$ – H]$^-$, 457 [$OsCl_2$(Hbzim)(dm*so*) – H]$^-$. IR (CsI): $\tilde{\nu}$ = 217 sh and 267 m ν(Os–N) and σ(Os–N–C); 288 and 320 m ν(Os–Cl); 389 m σ (C–S–O); 433, 462 sh and 471 sh s ν(Os–S); 964, 975, 1012, 1073, 1033 sh and 1097 vs ν(*S*–O); 1243, 1273, 1302, 1322 sh, 1423, 1465, 1486, 1498, 1595 and 1618 m ν(C–C), ν(C–N) and σ(C–H); 2932 and 3036 sh m ν(C–H); 3153 and 3453 b cm^{-1} w ν(N–H). UV/Vis (MeOH): λ_{max} (ε) = 274 nm (23288 M^{-1} cm^{-1}), 278 (23744). ^{1}H NMR (400.13 MHz, [D$_6$]dmso): δ = 13.18 (s, 1 H, NH), 8.78 (s, 1 H, CH=N), 8.21 (d, *J* = 8.1 Hz, 1 H, C4-H), 7.59 (d, *J* = 7.1 Hz, 1 H, C7-H), 7.29 (t, *J* = 7.2 Hz, 1 H, C6-H), 7.24 (t, *J* = 7.0 Hz, 1 H, C5-H), 3.59 (s, 6 H, CH_3), 3.45 (s, 6 H, CH_3), 3.28 (s, 6 H, CH_3) ppm. ^{13}C{^{1}H} NMR (100.62 MHz, [D$_7$]DMF): δ = 156.4 (C2), 141.4 (C8 or C9), 133.2 (C8 or C9), 123.7 (C6), 122.1 (C5), 122.1 (C4), 113.1 (C7), 48.9 (CH_3), 47.1 (CH_3), 45.7 (CH_3) ppm. X-ray diffraction quality crystals were obtained from a solution of **7** in ethanol.

***cis*,*fac*-[$OsCl_2$(Him)(dm*so*)$_3$] (8). Method (a):** Imidazole (0.036 g, 0.53 mmol) was added to a solution of *cis*-[$OsCl_2$(dmso)$_4$] (0.15 g, 0.26 mmol) in dry ethanol (20 mL) and the reaction mixture heated at 80 °C for 2 h. The solution volume was reduced to approximately 1 mL, the white solid was filtered off, washed with ethanol (2 × 2 mL) and dried in vacuo. Yield: 0.068 g (46%).

Method (b): A solution of **4** (0.08 g, 0.11 mmol) in dimethyl sulfoxide (2.5 mL) was heated slowly to 125 °C and maintained at this temperature for 2 h. The solvent was removed under reduced pressure and the white residue washed with a small amount of absolute ethanol and diethyl ether and dried in vacuo. Yield: 0.06 g (74%). $C_9H_{22}Cl_2N_2O_3OsS_3$ (563.61): calcd. C 19.17, H 3.93, N 4.97, S 17.06; found C 19.29, H 3.92, N 4.98, S 16.77. MS (ESI$^+$): *m/z* 587 [M + Na]$^+$; (ESI$^-$): *m/z* 563 [M – H]$^-$. IR (CsI): $\tilde{\nu}$ = 210 sh, 235 sh and 265 sh m ν(Os–N) and σ(Os–N–C); 280 and 299 m ν(Os–Cl); 393 m σ (C–S–O); 440 and 465 sh s ν(Os–S); 929, 974, 1015, 1062, 1073 sh and 1091 vs ν(*S*–O); 1261, 1300, 1316, 1413, 1451, 1490 and 1507 m ν(C–C), ν(C–N) and σ(C–H); 2929 and 3164 w ν(C–H); 3164 and 3292 cm^{-1} m ν(N–H). UV/Vis (MeOH): λ_{max} (ε) = 212 nm (1946 M^{-1} cm^{-1}), 215 (1992), 293 (1694). ^{1}H NMR (400.13 MHz, [D$_6$]dmso): δ = 12.62 (s, 1 H, NH), 8.35 (s, 1 H,

CH=N), 7.49 (s, 1 H, C4-H), 7.15 (s, 1 H, C5-H), 3.51 (s, 6 H, CH_3), 3.45 (s, 6 H, CH_3), 3.25 (s, 6 H, CH_3) ppm.$^{13}C\{^1H\}$ NMR (100.62 MHz, D_2O): δ = 140.2 (C2), 130.2 (C4), 117.0 (C5), 48.5 (CH_3), 47.2 (CH_3), 46.0 (CH_3) ppm. Crystals of **8**·C_2H_5OH suitable for X-ray data collection were obtained from a solution of **8** in ethanol.

Catalytic Hydration of Chloronitriles by a Metal Complex in Solution: Typically, a solution/suspension of [$Os^{II}Cl_2$(azole)$_2$(dm*so*)$_2$] or [$Os^{II}Cl_2$(azole)(dm*so*)$_3$] (ca. 10 mg) in a mixture of chloronitrile (1 mL) and water (1.3 mL) was stirred at 75 °C for 24 h in a Schlenk flask equipped with a magnetic stirring bar. The metal complex:chloronitrile and chloronitrile:water molar ratios were 1:600 and 1:7, 1:650 and 1:6, 1:760 and 1:6 for trichloroacetonitrile, dichloroacetonitrile and chloroacetonitrile, respectively. Control experiments regarding hydration of the corresponding chloronitrile were carried out under similar conditions but in the absence of the osmium(II) complex. In all cases solvents were removed under reduced pressure and at moderate temperature (≤40 °C) to avoid sublimation of the carboxamide. The amount of product was determined by ^1H NMR experiments in [D_6]dmso by using 1,3,5-trimethoxybenzene as internal reference. The following lines were integrated: CCl_3CONH_2: δ = 8.35 (d, $J_{N,H}$ = 46.5 Hz) ppm; CCl_3COONH_4: δ = 7.12 (t, $J_{N,H}$ = 51.1 Hz) ppm; $CHCl_2CONH_2$: δ = 7.80 (d, $J_{N,H}$ = 82.1 Hz), 6.32 (s, H, $CHCl_2$) ppm; $CHCl_2COONH_4$: δ = 7.12 (t, $J_{N,H}$ = 50.1 Hz) ppm; $CH_2ClCONH_2$: δ = 7.50 (d, $J_{N,H}$ = 103.3 Hz), 4.02 (s, 2 H, CH_2Cl) ppm; $CH_2ClCOONH_4$: δ = 7.22 (t, $J_{N,H}$ = 51.1 Hz) ppm; C_6H_3-(OCH_3)$_3$: δ = 6.08 (s, 3 H), 3.70 (s, 9 H) ppm.

Physical Measurements: Elemental analyses were carried out with a Carlo–Erba microanalyser at the Microanalytical Laboratory of the University of Vienna. Electrospray ionisation mass spectra were recorded with a Bruker esquire$_{3000}$ ion-trap mass spectrometer equipped with an orthogonal electrospray interface (Bruker Daltonics, Bremen, Germany) in both positive- and negative-ion modes. The Bruker Daltonics esquire 5.2 software bundle consisting of Bruker esquire Control 5.2 and Bruker Data Analysis 3.2 was used for acquiring spectra and data analysis, respectively. The sample solution in methanol was delivered at a flow rate of 3 μL min^{-1} using a syringe pump 74900 from Cole–Parmer Instrument Company (Vernon Hills, IL, USA); N_2 was used as both drying and nebulising gas (flow rate: 5 L min^{-1}). Expected and experimental isotope distributions were compared. IR spectra were obtained from CsI pellets with a Perkin–Elmer FT-IR 2000 instrument (4000–200 cm^{-1}). UV/Vis spectra were recorded with a Perkin–Elmer Lambda 20 UV/Vis spectrophotometer from samples dissolved in methanol. ^1H NMR spectra were recorded with a Bruker DPX400 (Ultrashield™ Magnet) spectrometer at 298 K. The residual ^1H present in $CDCl_3$ ([D_6]dmso, [D_7]DMF, D_2O) was

Table 6. Crystal data and details of data collection for **1**–**8**.

	1	**2**	**3**	**4**
Formula	$C_{18}H_{26}Cl_2N_4O_3OsS_2$	$C_{10}H_{20}Cl_2N_4O_2OsS_2$	$C_{20}H_{27}Cl_2N_5O_2OsS_2$	$C_{10}H_{20}Cl_2N_4O_2OsS_2$
Fw	671.65	553.52	694.69	553.52
Space group	$P2_1/n$	$P2_1/n$	$P2_1/n$	Cc
a [Å]	23.386(5)	8.796(2)	10.1853(2)	12.2467(2)
b [Å]	11.732(2)	16.397(3)	20.7233(5)	9.3749(2)
c [Å]	17.422(3)	12.266(2)	12.3821(3)	16.4373(3)
β [°]	103.04(3)	104.61(3)	95.416(1)	106.753(1)
V [Å^3]	4656.7(15)	1711.9(6)	2601.86(10)	1807.09(6)
Z	8	4	4	4
λ [Å]	0.71073	0.71073	0.71073	0.71073
ρ_{calcd} [g cm^{-3}]	1.916	2.148	1.773	2.035
Crystal size [mm]	0.22 × 0.22 × 0.17	0.20 × 0.14 × 0.11	0.17 × 0.11 × 0.09	0.19 × 0.16 × 0.14
T [K]	120	120	296	296
μ [cm^{-1}]	59.13	80.12	52.93	75.90
R_1[a]	0.0280	0.0174	0.0351	0.0261
wR_2[b]	0.1088	0.0425	0.0673	0.0602
GOF[c]	1.007	1.089	0.973	1.016
	5	**6**	**7**	**8**
Formula	$C_{15}H_{30}Cl_2N_2O_4OsS_3$	$C_9H_{22}Cl_2N_2O_3OsS_3$	$C_{13}H_{24}Cl_2N_2O_3OsS_3$	$C_{11}H_{28}Cl_2N_2O_4OsS_3$
Fw	659.69	563.57	613.62	609.63
Space group	$Pca2_1$	$P2_1$	$P2_1/c$	$P2_1/n$
a [Å]	14.242(3)	8.403(2)	10.1946(4)	8.467(2)
b [Å]	7.940(2)	12.965(3)	11.9361(5)	21.599(4)
c [Å]	19.685(4)	8.858(2)	15.9305(6)	10.851(2)
β [°]		117.33(3)	90.298(2)	91.60(3)
V [Å^3]	2226.0(9)	857.3(3)	1938.46(13)	1983.6(7)
Z	4	2	4	4
λ [Å]	0.71073	0.71073	0.71073	0.71073
ρ_{calcd} [g cm^{-3}]	1.968	2.183	2.103	2.041
Crystal size [mm]	0.23 × 0.20 × 0.12	0.16 × 0.14 × 0.13	0.17 × 0.08 × 0.06	0.23 × 0.17 × 0.09
T [K]	120	120	296	120
μ [cm^{-1}]	62.74	81.20	71.92	70.31
R_1[a]	0.0201	0.0204	0.0272	0.0205
wR_2[b]	0.0464	0.0471	0.0538	0.0503
GOF[c]	1.048	1.045	1.019	1.072

[a] $R_1 = \Sigma||F_o| - |F_c||/\Sigma|F_o|$. [b] $wR_2 = \{\Sigma[w\,(F_o^2 - F_c^2)^2]/\Sigma[w(F_o^2)^2]\}^{1/2}$. [c] GOF = $\{\Sigma[w(F_o^2 - F_c^2)^2]/(n - p)\}^{1/2}$, where *n* is the number of reflections and *p* is the total number of parameters refined.

used as internal reference. The assignment was confirmed by 2D NMR ($^{13}C,^{1}H$; $^{1}H,^{1}H$ and $^{13}C,^{1}H$ via long-range couplings) and NOE (1D and 2D) spectroscopy. Cyclic voltammograms were measured in a three-electrode cell using a 0.2-mm-diameter platinum disc working electrode, a platinum auxiliary electrode and an $Ag|Ag^{+}$ reference electrode containing 0.1 M $AgNO_3$. Measurements were performed at room temperature using an EG&G PARC 273A potentiostat/galvanostat. Deaeration of solutions was accomplished by passing a stream of argon through the solution for 5 min prior to the measurement and then maintaining a blanket atmosphere of argon over the solution during the measurement. The potentials were measured in 0.15 M $[n\mathrm{Bu_4N}][\mathrm{BF_4}]/\mathrm{CH_3CN}$ (dmf) using $[\mathrm{Fe}(\eta^5\text{-}\mathrm{C_5H_5})_2]$ ($E_{1/2}^{ox}$ = +0.69 V vs. NHE)[42] as internal standard, and are quoted relative to NHE.

Crystallographic Structure Determination: X-ray diffraction measurements were performed with a Nonius Kappa CCD and X8AP-EXII CCD diffractometers. Single crystals were positioned at 35, 30, 40, 40, 35, 30, 40 and 35 mm from the detector, and 620, 344, 1001, 1089, 404, 344, 1885 and 538 frames were measured, each for 15, 30, 60, 60, 10, 10, 60 and 30 s over a 1, 2, 0.5, 0.5, 2, 2, 0.5 and 1.5° scan width for **1**–**8**, respectively. The data were processed using the Denzo-SMN or SAINT-Plus software package.[43,44] Crystal data, data collection parameters and structure-refinement details for **1**–**8** are given in Table 6. The structures were solved by direct methods and refined by full-matrix least-squares techniques. Non-hydrogen atoms were refined with anisotropic displacement parameters. H atoms were placed in geometrically calculated positions and refined as riding atoms in the subsequent least-squares model refinements. The isotropic thermal parameters were estimated to be 1.2-times the values of the equivalent isotropic thermal parameters of the atoms to which hydrogens are bonded. The following computer programs were used: structure solution: SHELXS-97;[45] refinement: SHELXL-97;[46] molecular diagrams: ORTEP;[47] computer CPU: Pentium® IV; scattering factors were taken from the literature.[48]

CCDC-606815 (for **1**), -606816 (for **2**), -606811 (for **3**), -606814 (for **4**), -606817 (for **5**), -606818 (for **6**), -606813 (for **7**) and -606812 (for **8**) contain the supplementary crystallographic data for this paper. These data can be obtained free of charge from The Cambridge Crystallographic Data Centre via www.ccdc.cam.ac.uk/data_request/cif.

Supporting Information (see also the footnote on the first page of this article): ORTEP view of the second independent molecule 1B (Figure S1); cyclic voltammograms of complexes **1** and **3**–**8** (Figures S2–S8).

Acknowledgments

The authors are indebted to FWF and COST for financial support. We also thank Prof. G. Giester and Mr. A. Roller for X-ray data collection, and Dr. M. Galanski for NMR measurements. Dr. S. Shova and Mr. N. A. Sheddan are acknowledged for stimulating discussions.

[1] J. A. Davies, *Adv. Inorg. Chem. Radiochem.* **1981**, *24*, 115–187.
[2] H. B. Kagan, B. Ronan, *Rev. Heteroat. Chem.* **1992**, *7*, 92–116.
[3] M. Calligaris, O. Carugo, *Coord. Chem. Rev.* **1996**, *153*, 83–154.
[4] M. Calligaris, *Coord. Chem. Rev.* **2004**, *248*, 351–375.
[5] E. Alessio, *Chem. Rev.* **2004**, *104*, 4203–4242.
[6] G. Sava, E. Alessio, A. Bergamo, G. Mestroni, in *Topics in Biological Inorganic Chemistry*: *Metallo-Pharmaceuticals* (Eds.: M. J. Clarke, P. J. Sadler), Springer, Berlin, **1999**, vol. 1, p. 143–169.
[7] E. Alessio, G. Mestroni, A. Bergamo, G. Sava, in *Metal Ions in Biological Syst*ems: *Metal Complexes in Tumour Diagnosis and as Anticancer Agents* (Eds.: A. Sigel, H. Sigel, M. Dekker), New York, **2004**; vol. 42, p. 323–351.
[8] a) D. P. Riley, M. R. Thompson, J. Lyon III, *J. Coord. Chem.* **1988**, *19*, 49–59; b) R. S. Srivastava, *Appl. Organomet. Chem.* **2001**, *15*, 769–771; c) H. B. Henbest, J. Trocha-Grimshaw, *J. Chem. Soc., Perkin Trans. 1* **1974**, 607–608.
[9] a) M. Bressan, L. Forti, A. Morvillo, *J. Mol. Catal.* **1993**, *84*, 59–66; b) M. Bressan, L. Forti, F. Ghelfi, A. Morvillo, *J. Mol. Catal.* **1993**, *79*, 85–93; c) F. Porta, C. Crotti, S. Cenini, G. Palmisano, *J. Mol. Catal.* **1989**, *50*, 333–341.
[10] a) N. N. Dass, S. R. Sen, *J. Polym. Sci.* **1983**, *21*, 3381–3388; b) R. Castarlenas, I. Alaoui-Abdallaoui, D. Sémeril, B. Mernari, S. Guesmi, P. H. Dixneuf, *New J. Chem.* **2003**, *27*, 6–8; c) K. Kashiwagi, R. Sugise, T. Shimakawa, T. Matuura, M. Shirai, F. Kakiuchi, S. Murai, *Organometallics* **1997**, *16*, 2233–2235.
[11] a) P. K. L. Chan, K. A. Skov, B. R. James, N. P. Farrell, *Int. J. Radiat. Oncol. Biol. Phys.* **1986**, *12*, 1059–1062; b) P. K. L. Chan, K. A. Skov, B. R. James, *Int. J. Radiat. Biol.* **1987**, *52*, 49–55; c) P. K. L. Chan, P. K. H. Chan, D. C. Frost, B. R. James, K. A. Skov, *Can. J. Chem.* **1988**, *66*, 117–122; d) P. K. L. Chan, B. R. James, D. C. Frost, P. K. H. Chan, H.-L. Hu, K. A. Skov, *Can. J. Chem.* **1989**, *67*, 508–516.
[12] M. Henn, E. Alessio, G. Mestroni, M. Calligaris, W. M. Attia, *Inorg. Chim. Acta* **1991**, *187*, 39–50.
[13] M. Iwamoto, E. Alessio, L. G. Marzilli, *Inorg. Chem.* **1996**, *35*, 2384–2389.
[14] E. Alessio, E. Iengo, E. Zangrando, S. Geremia, P. A. Marzilli, M. Calligaris, *Eur. J. Inorg. Chem.* **2000**, 2207–2219.
[15] a) E. Alessio, M. Calligaris, M. Iwamoto, L. G. Marzilli, *Inorg. Chem.* **1996**, *35*, 2538–2545; b) L. G. Marzilli, M. Iwamoto, E. Alessio, L. Hansen, M. Calligaris, *J. Am. Chem. Soc.* **1994**, *116*, 815–816.
[16] a) M. M. T. Khan, P. S. Roy, K. Venkatasubramanian, N. H. Khan, *Inorg. Chim. Acta* **1990**, *176*, 49–55; b) M. M. T. Khan, N. M. Khan, R. I. Kureshy, K. Venkatasubramanian, *Polyhedron* **1992**, *11*, 431–441.
[17] E. Reisner, V. B. Arion, A. Rufińska, I. Chiorescu, W. F. Schmid, B. K. Keppler, *Dalton Trans.* **2005**, 2355–2364.
[18] E. Alessio, B. Serli, E. Zangrando, M. Calligaris, N. S. Panina, *Eur. J. Inorg. Chem.* **2003**, 3160–3166.
[19] A. J. Barton, W. Levason, G. Reid, V.-A. Tolhurst, *Polyhedron* **2000**, *19*, 235–240.
[20] T. Even, A. R. J. Genge, A. M. Hill, N. J. Holmes, W. Levason, M. Webster, *J. Chem. Soc., Dalton Trans.* **2000**, 655–662.
[21] A. M. McDonagh, M. G. Humphrey, D. C. R. Hockless, *Tetrahedron: Asymmetry* **1997**, *8*, 3579–3583.
[22] D. A. Freedman, D. J. Magneson, K. R. Mann, *Inorg. Chem.* **1995**, *34*, 2617–2624.
[23] E. Reisner, V. B. Arion, A. Eichinger, N. Kandler, G. Giester, A. J. L. Pombeiro, B. K. Keppler, *Inorg. Chem.* **2005**, *44*, 6704–6716.
[24] M. F. C. G. Guedes da Silva, A. J. L. Pombeiro, S. Geremia, E. Zangrando, M. Calligaris, A. V. Zinchenko, V. Yu. Kukushkin, *J. Chem. Soc., Dalton Trans.* **2000**, 1363–1371.
[25] A. B. P. Lever, *Inorg. Chem.* **1990**, *29*, 1271–1285.
[26] V. Yu. Kukushkin, A. J. L. Pombeiro, *Chem. Rev.* **2002**, *102*, 1771–1802.
[27] M. Hashimoto, K. Hamada, K. Mano, *Bull. Chem. Soc. Jpn.* **1987**, *60*, 1924–1926.
[28] E. A. Shomova, V. P. Rudavskii, I. G. Khaskin, *Mikrobiologiya* **1965**, *34*, 715–719.
[29] M. Nagasawa, M. Yoshido, R. Kubota, JP 32008650 19571007, **1957**.
[30] H. C. Englert, U. Gerlach, D. Mania, W. Linz, H. Gögelein, E. Klaus, P. Crause, EP 779288 A1 19970618, **1997**.

[31] D. Uemura, K. Yamada, A. Yamada, K. Suenaga, A. Takada, JP 11322593 A2 19991124, **1999**.
[32] P. C. Hamm, US Pat. 67-639657 19670519, **1971**.
[33] N. Komaki, Y. Hoshika, H. Taya, A. Fujinami, Y. Asano, N. Kameda, DE 2232176 19730111, **1973**.
[34] a) J. Quirante, C. Escolano, F. Diaba, J. Bonjoch, *J. Chem. Soc., Perkin Trans. 1* **1999**, 1157–1162; b) T. Nishikawa, N. Ohyabu, N. Yamamoto, M. Isobe, *Tetrahedron* **1999**, *55*, 4325–4340; c) N. Yamamoto, M. Isobe, *Chem. Lett.* **1994**, 2299–2302; d) A. J. Speziale, R. C. Freeman, *J. Am. Chem. Soc.* **1960**, *82*, 903–909.
[35] a) D. Albanese, D. Landini, M. Penso, *J. Org. Chem.* **1992**, *57*, 1603–1605; b) S. Takano, K. Ogasawara, M. Akyama, JP 61022053 A2 19860130, **1986**.
[36] a) E. B. Dol'berg, G. I. Kovalenko, B. G. Yasnitskii, *Metody Poluch. Khim. Reaktiv. Prep.* **1970**, 116–118; b) K. Maruyama, JP 44028889 19691126, **1969**; c) G. Popov, I. Knape, P. Mann, K. Peters, C. Pöschl, DE 10218603 A1 20031120, **2003**.
[37] N. V. Kaminskaia, N. M. Kostić, *J. Chem. Soc., Dalton Trans.* **1996**, 3677–3686.
[38] V. Yu. Kukushkin, A. J. L. Pombeiro, *Inorg. Chim. Acta* **2005**, *358*, 1–21.
[39] F. Matsuda, *Chemtech* **1977**, *7*, 306–308.
[40] E. Cariati, C. Dragonetti, L. Manassero, D. Roberto, F. Tessore, E. Lucenti, *J. Mol. Catal. A* **2003**, *204–205*, 279–285.
[41] L. Heinrich, A. Mary-Verla, Y. Li, J. Vaissermann, J.-C. Chottard, *Eur. J. Inorg. Chem.* **2001**, 2203–2206.
[42] W. C. Barrette Jr., H. W. Johnson Jr., D. T. Sawyer, *Anal. Chem.* **1984**, *56*, 1890–1898.
[43] Z. Otwinowski, W. Minor, in *Macromolecular Crystallography, Part A* (Eds.: C. W. Jr., Carter, R. M. Sweet), Academic Press, New York, **1997**, vol. 276, p. 307–326.
[44] SAINT-Plus (Version 7.06a) and APEX2, Bruker-Nonius AXS Inc. **2004**, Madison, Wisconsin, USA.
[45] G. M. Sheldrick, SHELXS-97, Program for Crystal Structure Solution, **1997**, University of Göttingen, Germany.
[46] G. M. Sheldrick, SHELXL-97, Program for Crystal Structure Refinement, **1997**, University of Göttingen, Germany.
[47] G. K. Johnson, Report ORNL-5138, Oak Ridge National Laboratory, Oak Ridge, TN, **1976**.
[48] *International Tables for X-ray Crystallography*, Kluwer Academic Press, Dordrecht, The Netherlands, **1992**; vol. C, Tables 4.2.6.8 and 6.1.1.4.9.

Received: September 14, 2006
Published Online: November 21, 2006

